Received: 4 February 2020 | Revised: 5 October 2020 | Accepted: 7 October 2020

DOI: 10.1111/cas.14691

ORIGINAL ARTICLE

Cancer Science WILEY

Inactivation of homeodomain-interacting protein kinase 2 promotes oral squamous cell carcinoma metastasis through inhibition of P53-dependent E-cadherin expression

Xueqing Zheng[1,2] | Yuemei Pan[1,2,3] | Xinming Chen[1,2] | Shu Xia[1,2] | Yaying Hu[1,2] | Yi Zhou[1] | Jiali Zhang[1,2]

[1]The State Key Laboratory Breeding Base of Basic Science of Stomatology (Hubei_MOST) and Key Laboratory of Oral Biomedicine Ministry of Education, School and Hospital of Stomatology, Wuhan University, Wuhan, China

[2]Oral Histopathology Department, School and Hospital of Stomatology, Wuhan University, Wuhan, China

[3]Stomatological Hospital, Southern Medical University, Guangzhou, China

Correspondence
Jiali Zhang and Yi Zhou, Hubei_MOST & Key Laboratory of Oral Biomedicine Ministry of Education, School & Hospital of Stomatology, Wuhan University, Wuhan, China.
Emails: jiali_zhang@whu.edu.cn (J.Z.); dryizhou@163.com (Y.Z.)

Funding information
National Natural Science Foundation of China, Grant/Award Number 81572664.

Abstract

Homeodomain-interacting protein kinase 2 (HIPK2), a well-known tumor suppressor, shows contradictory expression patterns in different cancers. This study was undertaken to clarify HIPK2 expression in oral squamous cell carcinoma (OSCC) and to reveal the potential mechanism of HIPK2 involvement in OSCC metastasis. Two hundred and four OSCC tissues, together with paired adjacent normal epithelia, dysplastic epithelia, and lymph node metastasis specimens, were collected to profile HIPK2 expression by immunohistochemical staining. High throughput RNA-sequencing was used to detect the dysregulated signaling pathways in HIPK2-deficient OSCC cells. Transwell assay and lymphatic metastatic orthotopic mouse model assay were undertaken to identify the effect of HIPK2 on tumor invasion. Western blotting and luciferase reporter assay were used to examine the HIPK2/P53/E-cadherin axis in OSCC. Nuclear delocalization of HIPK2 was observed during oral epithelial cancerization progression and was associated with cervical lymph node metastasis and poor outcome. Depletion of HIPK2 promoted tumor cell invasion in vitro and facilitated cervical lymph node metastasis in vivo. According to mRNA-sequencing, pathways closely related to tumor invasion were notably activated. Homeodomain-interacting protein kinase 2 was found to trigger E-cadherin expression by mediating P53, which directly targets the *CDH1* (coding E-cadherin) promoter. Restoring P53 expression rescued the E-cadherin suppression induced by HIPK2 deficiency, whereas rescued cytoplasmic HIPK2 expression had no influence on the expression of E-cadherin and cell mobility. Together, nuclear delocalization of HIPK2 might serve as a valuable negative biomarker for poor prognosis of OSCC and lymph node metastasis. The depletion of HIPK2 expression promoted OSCC metastasis by suppressing the P53/E-cadherin axis, which might be a promising target for anticancer therapies.

KEYWORDS

E-cadherin, HIPK2, invasion, oral squamous cell carcinoma, subcellular localization

Xueqing Zheng and Yuemei Pan contributed equally to this work.

1 | INTRODUCTION

Oral squamous cell carcinoma (OSCC) is one of the most common and aggressive epithelial malignancies,[1] 30%-50% of which show early lymph node metastasis during clinical examination.[2-6] Therefore, the investigation of specific biomarkers that indicate OSCC metastasis and prognosis is critical for OSCC treatment.[7]

Homeodomain-interacting protein kinase 2 (HIPK2), an evolutionarily conserved nuclear serine/threonine kinase, acts as a corepressor of transcriptional regulators and is closely related to tumorigenesis.[8-10] This protein can modulate a wide spectrum of biological functions such as growth, cell death, DNA damage response, apoptosis, cell proliferation, and invasion.[8,11-14] Previous studies have shown that HIPK2 expression is decreased in a variety of cancers[15-18] and that it inhibits tumor invasion[15] and growth,[9,18,19] and promotes apoptosis.[17] However, HIPK2 is also reported to be significantly increased in tumors such as pilocytic astrocytoma,[20] the solid subtype of basal cell carcinoma[21] and cervical cancer,[22] and could promote cell growth and apoptosis. These seemingly contradictory results suggest that HIPK2 plays different roles in various types of human cancers and imply that the total amount of HIPK2 in cancer is not the only determinant of HIPK2 kinase activity. Studies have also reported that, in some pathological conditions, HIPK2 is inactivated by loss of this kinase in the nucleus (termed nuclear delocalization), shifts its localization to the cytoplasm (cytoplasmic relocalization) through reactive oxygen species-induced acetylation, phosphorylation, or autophosphorylation[23,24] and protects tumor cells from cell death.[10,23,25-28] However, the clarification of the subcellular localization and potential function of HIPK2 in OSCC tumorigenesis are largely unknown.

As an effective activator of P53, the classical role of HIPK2 is to respond to various stress signals, thus inducing cell cycle arrest and apoptosis.[29,30] Recently, emerging lines of evidence has suggested that HIPK2 might have other functions that oppose the epithelial-mesenchymal transition (EMT) process, and thus HIPK2 might inhibit tumor invasion and metastasis.[15,17,31-33] However, the mechanisms involved in HIPK2-mediated tumor invasion and metastasis have not been fully elucidated, and the signaling pathways vary in different cancer types. For example, HIPK2 knockdown could induce Wnt signaling activation and β-catenin nuclear localization, and thus promote EMT and subsequent cell invasion in bladder cancer.[15] In mammary tumors, the depletion of HIPK2 activates β_4 transcription, which results in a strong increase in β_4-dependent MAPK and Akt phosphorylation.[34] Moreover, HIPK2 overexpression directly downregulates vimentin expression, which correlates with impairment of breast cancer cell migration.[33]

To our knowledge, the role of HIPK2 in OSCC metastasis has not been clearly defined. In this study, we found that HIPK2 delocalized from the cell nucleus, which was associated with OSCC lymph node metastasis. Importantly, we described the effective function of HIPK2 in maintaining epithelial integrity by regulating P53-dependent E-cadherin (E-Cad) expression. This study could provide new insights into the mechanisms of HIPK2-mediated EMT signaling in OSCC.

2 | MATERIALS AND METHODS

2.1 | Clinical sample collection and tissue microarrays

In all, 204 paraffin-embedded OSCC tissues were obtained from OSCC patients undergoing primary surgery at the Stomatology Hospital of Wuhan University (Hubei, China) between 2002 and 2012. All samples of adjacent normal epithelia were obtained by local excision. The Ethics Committee of Wuhan University approved the examination of patient samples. The histological types and tumor grades were analyzed by two experienced pathologists. Among these samples, 99 cases of dysplastic epithelia were selected. Of these, 56 patients were determined to have cervical lymph node metastasis. By including cores from the above paraffin-embedded samples, tissue microarrays were designed and produced by Outdo Biotech (Shanghai, China).

2.2 | Immunohistochemical staining, scoring system, hierarchical clustering and data visualization

Immunohistochemical staining was carried out as previously described.[35] The primary Ab used was HIPK2 (1:500; Sigma). The immunohistochemically stained slides were scanned by an Aperio ScanScope CS scanner and analyzed by Aperio ImageScope version 11.2.0. Four random fields of interest were selected and quantified. The histoscore of HIPK2 staining in each field was calculated using the formula: (total intensity of strong positive × 3 + total intensity of positive × 2 + total intensity of weak positive × 1) / total cell numbers. The final histoscore = (field 1 + field 2 + field 3 + field 4) / 4. The hierarchical analysis was then carried out using HemI 1.0 software.

2.3 | Cell culture

The human immortalized oral epithelial cell line HIOEC was a gift from Professor Bian Zhuan (Wuhan University). The head and neck squamous cell carcinoma (SCC) cell lines (Cal-27, SCC-9, and SCC-25) and the HEK-293E embryonic kidney cell line were obtained from ATCC. The SCC cell lines UM-SCC-23 and HSC3 were gifts from Dr Thomas E. Carey (University of Michigan) and Professor Chen Qianming (Sichuan University), respectively. Cell lines were authenticated by Shanghai XP Biomed (Shanghai, China). Cal-27, UM-SCC-23, and HSC3 cells were cultured in DMEM medium (Hyclone), and HEK-293E cells were cultured in RPMI medium (HyClone). SCC-9 and SCC-25 cells were cultured in F12 medium (HyClone) supplemented with 400 ng/mL hydrocortisone. HIOEC cells were cultured in KBM medium (Lonza).

2.4 | Plasmids and transfection

For the HIPK2 knockdown study, the lentiviral vectors GV-248-HIPK2-sh1, GV-248-HIPK2-sh2, and sh-scramble plasmid were

purchased from Genechem and were verified by sequencing. For the HIPK2 overexpression study, the HIPK2 CDS sequence (NM_001113239.2) was PCR-amplified and inserted into the lentivirus vector PCDH-CMV-MCS-EF1-puro (Systems Biosciences). For the cytoplasmic HIPK2 expression rescue, the PCDH-CMV-MCS-EF1-puro-flag-HIPK2 plasmid was constructed by Miaoling Bioscience. Site-directed mutagenesis (HIPK2 KK776/778AA, HIPK2 R806A, and HIPK2 K808E) was done using the Mut Express II Fast Mutagenesis Kit V2 (Vazyme) according to the manufacturer's instructions. All the primer pairs are shown in Table S1. The PCDNA3-P53 plasmid (constructed by Miaoling Bioscience) was applied to rescue P53 expression. Lipofectamine 2000 (Invitrogen) was used for transient plasmid transfection.

2.5 | Cell invasion assay

For the cell invasion assay, an 8.0 μm thick chamber (Corning) was coated with 40 μL Matrigel (1:4, diluted in corresponding medium; BD Biosciences). In all, 5×10^5 cells were seeded in serum-free medium in the upper chamber, while the lower chamber was filled with 600 μL medium containing 20% FBS. After 48 hours of incubation, cells on the lower side of the chamber were fixed in 4% paraformaldehyde and stained with crystal violet. The total numbers of stained cells attached to the lower side of the membrane were counted under a microscope. Five fields were randomly selected to calculate the mean cell numbers.

2.6 | Lymphatic metastasis in an orthotopic mouse model of OSCC

Lymphatic metastasis in an orthotopic mouse model of OSCC was established according to a previous report.[36,37] Briefly, 6-8-week-old female BALB/c nude mice (Charles River) were randomly assigned to the sh-scramble or the HIPK2-knockdown group (n = 5) followed by injection of 1×10^6 cells into the right lateral tongue. Two weeks after injection, the mice were killed. Their cervical lymph nodes were isolated, measured (volume = length (the largest diameter) × width (the smallest diameter)^2 / 2), and serially sectioned for H&E staining. All procedures were approved by the animal ethics committee of Wuhan University and all mice were handled according to the guidelines of the Care and Use of Laboratory Animals (Ministry of Science and Technology of China, 2006).

2.7 | mRNA-sequencing

Total RNA was extracted using TRIzol (Invitrogen), which was then used for mRNA-sequencing (Sangon Biotech). The criterion for differential gene expression was set as |fold change| > 1.5 and false discovery rate less than 0.05. Gene Ontology (GO) analysis was carried out using KOBAS (version 2.0). The significance of GO term enrichment was analyzed using Fisher's exact test.

2.8 | Quantitative RT-PCR

Total RNA was isolated using the HP total RNA isolation kit (Omega Bio-Tek) following the manufacturer's instructions. Total RNA (1 μg) was reverse-transcribed into cDNA using a Takara RT reagent kit. Quantitative PCR was carried out using Roche FastStart Essential DNA Green Master (Roche) with the primers listed in Table S2. The cycling parameters were 95°C, 15 minutes; 40 cycles of (95°C, 15 seconds; 55°C, 30-40 seconds; and 72°C, 30 seconds). The relative gene expression was calculated using the equation $2^{-\Delta(\Delta Ct)}$ where $\Delta Ct = Ct\,(mRNA) - Ct\,(\beta\text{-actin})$.

2.9 | Protein extraction and western blot analysis

The total proteins were isolated from the OSCC cell lines using RIPA buffer (Beyotime) supplemented with 1 mmol/L PMSF (Beyotime) and Protease Inhibitor Cocktail Tablets (Roche). Proteins (40 μg) of different groups were boiled for 5 minutes in sample buffer, subjected to 10% SDS-PAGE and then electrophoretically transferred onto PVDF membranes. Nonspecific reactivity was blocked using 5% nonfat milk (Krbio) and then probed with primary Abs overnight at 4°C. Primary Abs used were as follows: HIPK2 (1:1000) purchased from Abcam, SNAI1 (1:1000) purchased from ABclonal, E-Cad (1:1000), WNT4 (1:500), P53 (1:1000), P53-Ser46 (1:1000), and β-actin (1:3000) purchased from Santa Cruz Biotechnology. Bound Abs were detected using HRP-conjugated secondary Ab (1:10 000; Santa Cruz Biotechnology). Triplicate experiments were undertaken to confirm the results. The immunoreactive proteins were detected by the ECL chemiluminescence system (Beyotime) and protein amounts were estimated through densitometry as the ratio detected protein / β-actin.

2.10 | Immunofluorescence and confocal microscopy

Cells were fixed, permeabilized, and blocked with 3% BSA. The primary Abs HIPK2 (1:500; Sigma), P53 (1:300; Santa Cruz Biotechnology), E-Cad (1:50; Santa Cruz Biotechnology) or flag (1:300; ABclonal) were incubated with the cells at 4°C overnight, followed by incubation with a fluorochrome-conjugated secondary Ab (ABclonal) for 1 hour. Cell nuclei were stained with DAPI. Immunofluorescence signals were recorded by confocal microscopy, and the mean integrated optical density was processed using Image-Pro Plus 6.0.

2.11 | Luciferase reporter assay

Four *CDH1* promoter fragments (Table S3) were amplified and inserted into dual-luciferase reporter vector pSiCheck-2 (Promega). Seed matching sequences were mutated with the Mut Express II

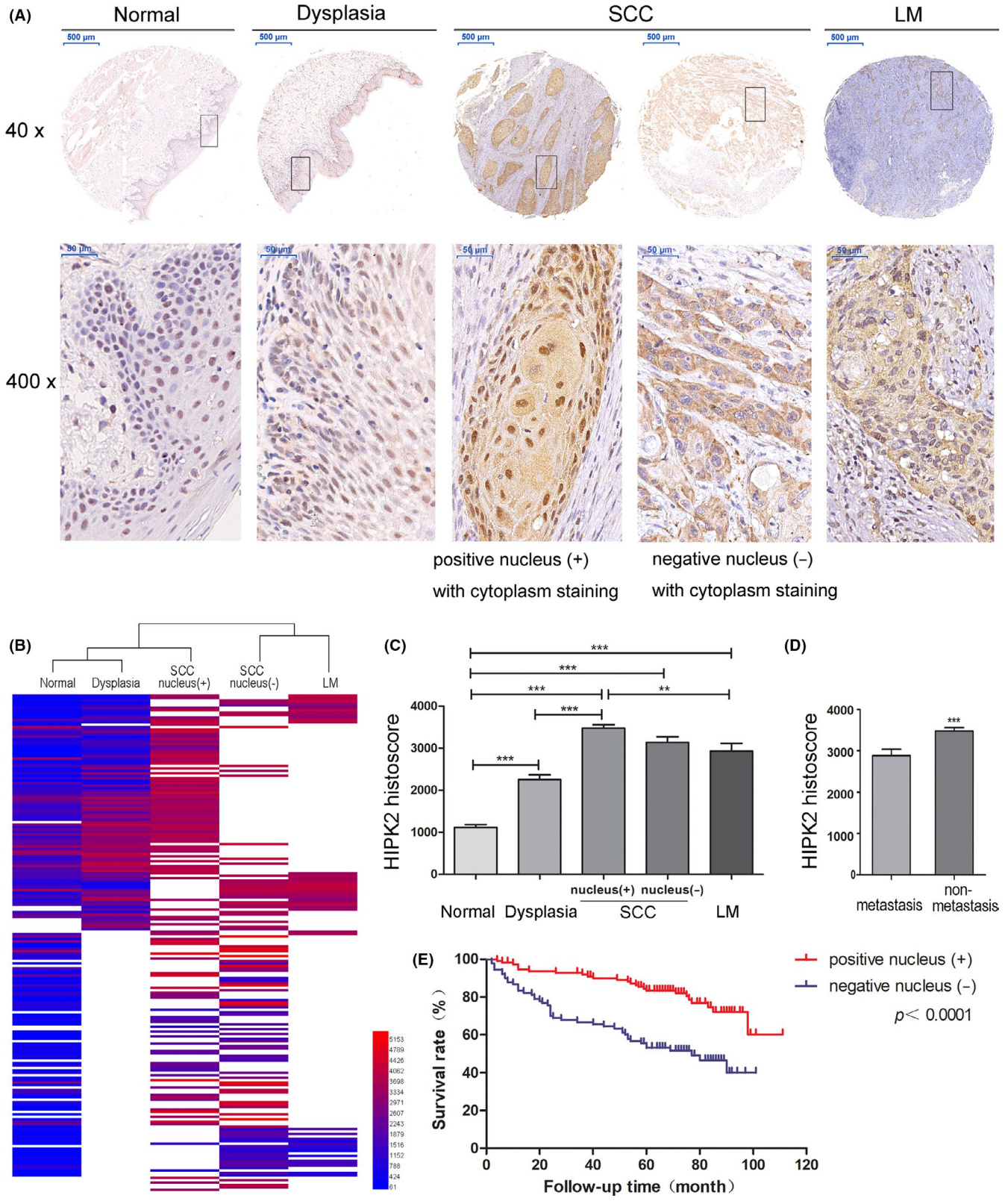

Fast Mutagenesis Kit V2 (Vazyme). Primer sets for the *CDH1* promoter fragments and the amplification of related mutant fragments are listed in Table S4. These constructed vectors were verified by sequencing. The luciferase activities were measured using a Dual-Luciferase Reporter Assay System (Promega). *Renilla* luciferase activity was normalized to firefly luciferase activity. The final normalized luciferase activity was normalized by pSiCheck-2-*CDH1* promoter / pSiCheck-2 or pSiCheck-2-*CDH1* mut promoter / pSiCheck-2.

FIGURE 1 Homeodomain-interacting protein kinase 2 (HIPK2) staining expression profile in oral squamous cell carcinoma (OSCC) tissues. A, Representative images of HIPK2 immunohistochemical staining in cores of adjacent normal epithelia, dysplastic epithelia, primary SCC, and lymph node metastases (LM). In the primary SCC, HIPK2 staining displayed two cellular localization patterns: nuclear localization (left) and nuclear delocalization (right). B, Hierarchical clustering analysis allowed for visualization of HIPK2 expression in adjacent normal epithelia, dysplastic epithelia, primary SCC, and LM in 204 OSCC cases. Columns and rows represent different tissue types and different cases, respectively. C, Histoscores of HIPK2 staining in dysplastic epithelia, primary SCC nuclei (+), primary SCC nuclei (−), and LM increased to 2.01-fold ($P < .001$), 3.11-fold ($P < .001$), 2.80-fold ($P < .001$), and 2.62-fold ($P < .001$), respectively, compared with adjacent normal epithelia. D, HIPK2 histoscores in nonmetastasis cases were 1.21 times higher than those in nonmetastasis cases ($P < .001$). E, Kaplan-Meier survival analysis showed that patients with negative nuclear HIPK2 expression were significantly more likely to have an unfavorable 5-y survival. $^{**}P < .01$; $^{***}P < .001$

2.12 | Statistical analysis

All data were represented as the mean ± SEM and were analyzed by GraphPad Prism 5. The overall survival rates were obtained by the Kaplan-Meier method and were compared by log-rank tests. Significant differences between dichotomous variables were tested by χ^2 tests. Analyses between two groups were determined using Student's *t* test. The correlation analysis between HIPK2 expression ratio of nucleus to cytoplasm, E-Cad expression, and P53 expression was carried out by Pearson's correlation. $P \leq .05$ was considered significant.

3 | RESULTS

3.1 | Nuclear delocalization of HIPK2 was observed during oral epithelial cancerization progression

Recent findings indicate that HIPK2 inhibition, aberrant localization, and overexpression exist in different tumors, with each leading to precisely opposite oncological outcomes.[15,16,21-23,26] Here, the characteristic of HIPK2 expression was comprehensively profiled in 204 OSCC tissues together with paired adjacent normal epithelia, dysplastic epithelia, and lymph node metastasis (LM) specimens (Figure 1A). There were HIPK2-positive and -negative cells in adjacent normal epithelia, and HIPK2 signals were observed in the nuclei. The expression became stronger in the nuclei of dysplastic epithelia, while slight cytoplasmic staining was also detected. Two types of HIPK2 cellular localization patterns were observed in primary SCC: 54.4% cases displayed intensively positive nuclei with cytoplasmic staining (nuclear localization) and 45.6% cases showed negative nuclei with cytoplasmic staining (nuclear delocalization/cytoplasmic relocalization). The HIPK2 expression pattern in the LM was compatible with that in the primary SCC, but the majority of SCC metastases (62.3%) showed nuclear delocalization. The hierarchical cluster analysis was used to categorize the negative nuclei OSCC group and the LM group into one subclass, which was robustly distinguished from the other three tissue groups (Figure 1B). Statistically, the histoscores of HIPK2 staining in dysplastic epithelia and cancer tissues were remarkably increased compared with those of the adjacent normal epithelia (Figure 1C, $P < .001$). A modest reduction in HIPK2 expression was detected in LM tissues compared with primary cancer tissues (Figure 1C). Moreover, the cases of metastasis showed lower HIPK2 staining scores than the cases of nonmetastasis (Figure 1D, $P < .001$).

3.2 | Nuclear delocalization of HIPK2 associated with unfavorable clinicopathological characteristics and patient survival

To investigate the effect of HIPK2 on OSCC prognosis, we analyzed the relationship between HIPK2 expression in primary OSCC and the clinicopathological characteristics. Statistically, nuclear delocalization of HIPK2 was closely correlated with advanced clinical stage ($P = .00004$), higher pathological grade ($P = .0071$), and greater tendency for lymph node metastasis ($P = .0046$; Table 1), and

TABLE 1 Relationship between the different homeodomain-interacting protein kinase 2 (HIPK2) expression modes in oral squamous cell carcinoma and the patients' clinicopathological characteristics

		HIPK2 expression modes		
Group	Cases	Positive nucleus (+)	Negative nucleus (−)	*P* value
Sex				
Male	119	64	55	.83070
Female	85	47	38	
Age, years				
<60	128	71	57	.69400
≥60	76	40	36	
Clinical stages[a]				
I-II	78	51	27	.00004***
III-IV	62	19	43	
Pathological grades				
I-II	156	93	63	.00710**
III	48	18	30	
Metastases				
M0	151	91	60	.00460**
M1	53	20	33	

[a]Among 204 patients, the clinical stages of 64 patients had not been recorded in their clinical data.

$^{**}P < .01$.

$^{***}P < .001$.

unfavorable 5-year survival ($P < .0001$; Figure 1E) compared with the nuclear localization group.

3.3 | Depletion of HIPK2 promoted tumor cell invasion in vitro

To validate whether the loss of HIPK2 function affected OSCC invasion, cell lines (UM-SCC-23, SCC-25, and Cal-27) in which HIPK2 was stably inhibited using two lentiviral vectors, GV-248-HIPK2-sh1 and -sh2, were constructed for the cell invasion assay (Figure 2A). As shown in Figure 2B, inhibition of HIPK2 expression significantly activated tumor cell invasion capability in vitro, which led to 1.72-2.78-fold increases compared with the sh-scramble group.

3.4 | HIPK2 facilitated cervical LM in vivo

To further elucidate the effect of HIPK2 deficiency on tumor metastasis in vivo, tumor cells were injected into the right lateral tongue of nude mice and then cervical lymph node metastasis was evaluated. Fourteen days after the injection, the average volume of lymph nodes in the Cal-27-HIPK2-sh2 group (6.70 ± 3.97 mm^3) was 1.80-fold larger than that of lymph nodes in the sh-scramble group (3.72 ± 2.10 mm^3) ($P < .001$; Figure 3A,B). Suppression of HIPK2 yielded higher ipsilateral LM frequencies (lymph node lesion-bearing animals / total animals used) and showed a tendency to give rise to multiple lymph node foci. In all, 100% (5/5) of the mice in the Cal-27-HIPK2-sh2 mice group developed metastasis, and six of 10 ipsilateral lymph nodes were metastatic. In comparison, LM was only detected in 40% (2/5) of the sh-scramble mice, and only two of 10 ipsilateral lymph nodes were metastatic (Figure 3C).

3.5 | mRNA-sequencing revealed signaling pathways associated with tumor invasion and EMT in HIPK2-attenuated cells

To explore the functional categories and canonical pathways that are dysregulated when HIPK2 is inhibited, RNA-sequencing and GO analyses were carried out in Cal-27-HIPK2-sh2 cells and Cal-27-sh-scramble cells. The pathways closely related to tumor invasion were significantly present in the enrichment pathways of differentially expressed genes. The top 10 enriched invasion-related pathways are listed in Figure 4A, and the top 10 specific related genes of each pathway were shown in Figure 4B. Among these genes, 15

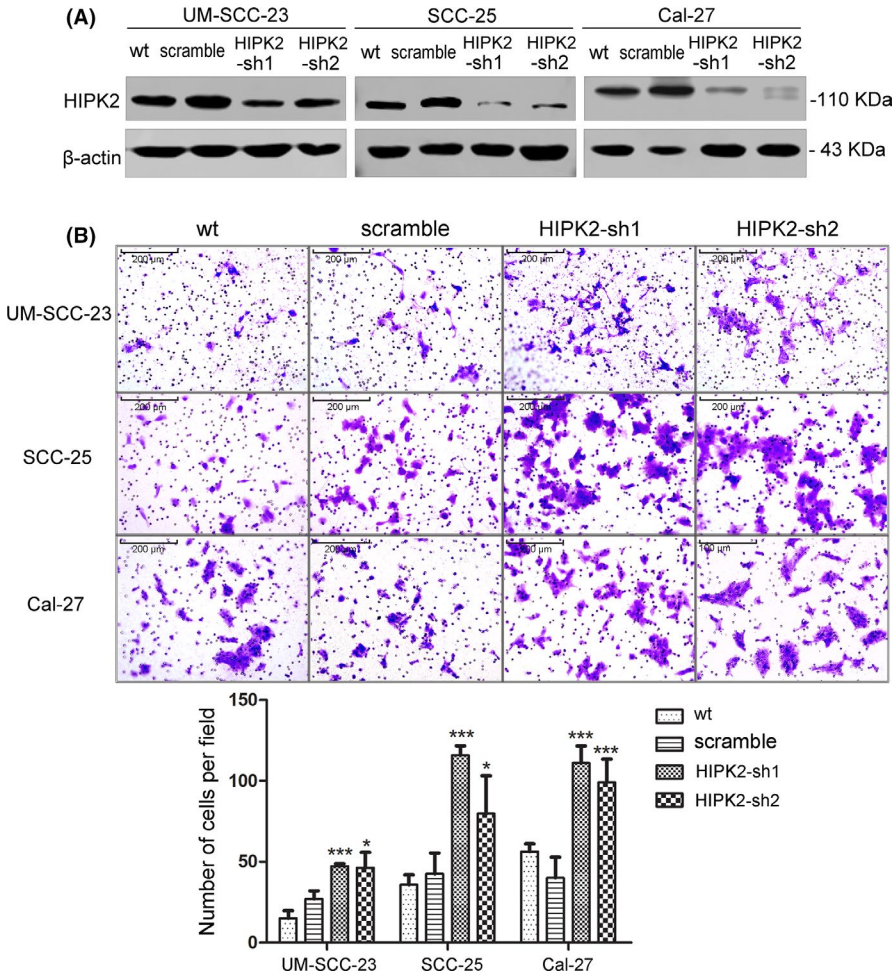

FIGURE 2 Attenuated homeodomain-interacting protein kinase 2 (HIPK2) expression promoted tumor cell invasion in vitro. A, HIPK2 protein expression was attenuated in UM-SCC-23, SCC-25, and Cal-27 cells by stably knocking down the *HIPK2*gene using two constructed lentiviral vectors, GV-248-HIPK2-sh1 and -sh2. B, Transwell assay showed that cell invasion capability was significantly increased in UM-SCC-23-/SCC-25-/Cal-27-HIPK2-shs cells compared with sh-scramble and wt cells. Original magnification, ×200. *$P < .05$; ***$P < .001$

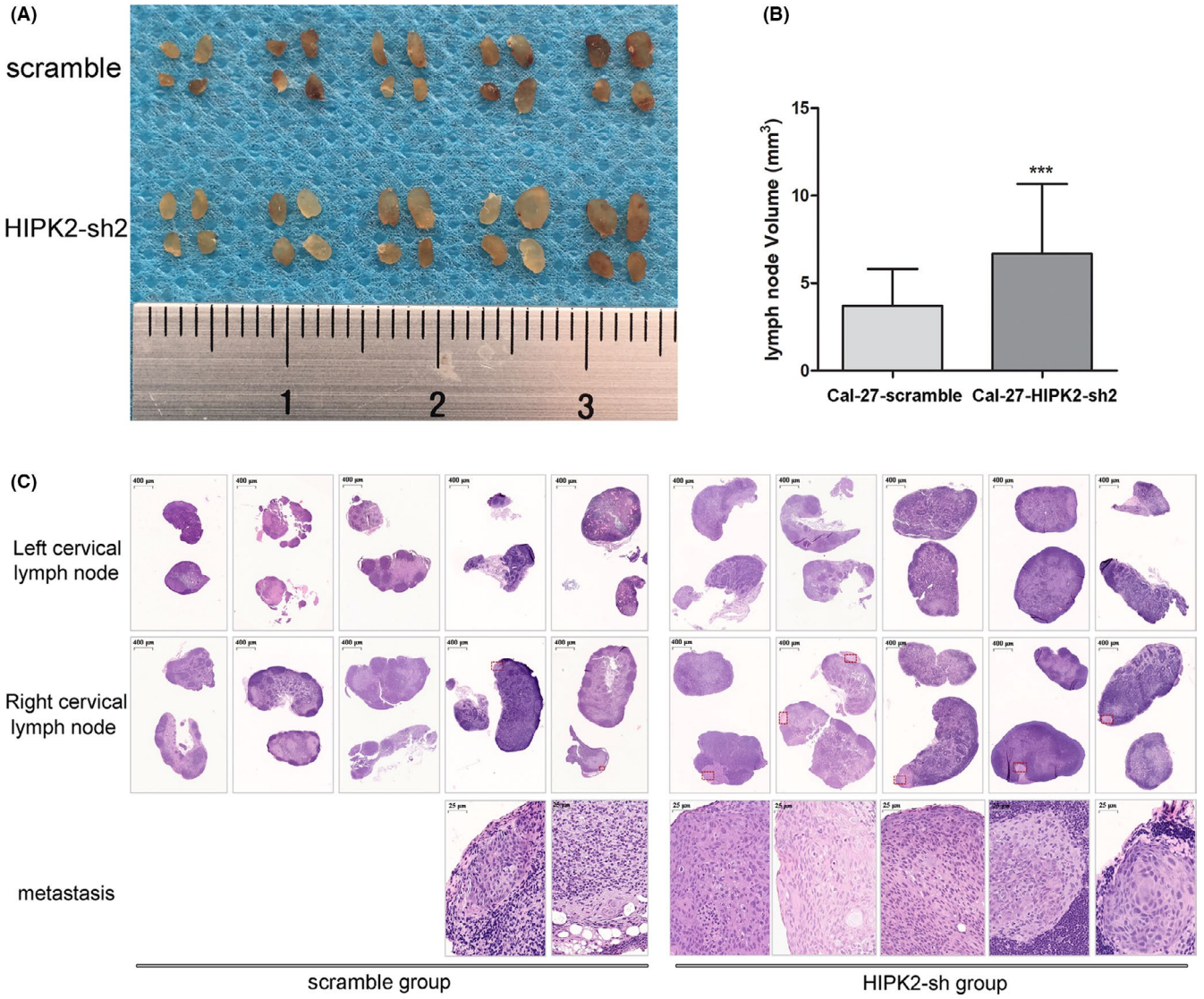

FIGURE 3 Inhibition of homeodomain-interacting protein kinase 2 (HIPK2) promoted cell invasion in vivo. A, Isolated cervical lymph nodes of BALB/c nude mice were injected with Cal-27-HIPK2-sh2 cells (bottom row) or Cal-27-sh-scramble cells (top row) into the right lateral tongue. For each mouse, four lymph nodes were isolated from the bilateral cervical area (two left and two right). B, Average volume of lymph nodes in the Cal-27-HIPK2-sh2 mice group and the sh-scramble group. C, Histological images of the isolated bilateral cervical lymph nodes (original magnification, ×25) and the corresponding metastatic areas in the sh-scramble group (left) and the Cal-27-HIPK2-sh2 group (right) (original magnification, ×400). ***$P < .001$

differentially expressed genes potentially related to HIPK2 deficiency-induced EMT were selected to undertake quantitative PCR assay (Figure S1). Then, five differentially expressed genes (*CDH1*, *WNT4*, *SNAI1*, *CLDN3*, and *PLEKHA7*) were identified in mRNA expression level, three of which were hallmark EMT genes (*CDH1*, *WNT4*, and *SNAI1*). Finally, only E-Cad (*CDH1*) was identified stably and remarkably decreased in protein level (Figure 5A).

3.6 | Expression of E-Cad and P53 regulated by HIPK2

To ascertain the underlying molecular mechanism of HIPK2 suppression involvement in tumor invasion, E-Cad identified in mRNA expression level was further investigated in two different OSCC cell lines using two distinct HIPK2-sh sequences. Notably, E-Cad showed the most obvious reduction in HIPK2-suppressed cells (Figure 5B), while forced HIPK2 expression led to a significant increase in E-Cad expression (Figure 5C). It is known that HIPK2 acts as an essential cotranscriptional regulator of P53 and can phosphorylate the P53 protein at N-terminal serine 46, which promotes P53-dependent gene expression.[29,30] Therefore, we examined the protein expression levels of P53 and P53-Ser46 in HIPK2-deficient tumor cells. The results showed that HIPK2 attenuation significantly decreased P53 and P53-Ser46 protein levels (Figure 5B). Inversely, forced HIPK2 expression reversed the expression of P53 and P53-Ser46 (Figure 5C).

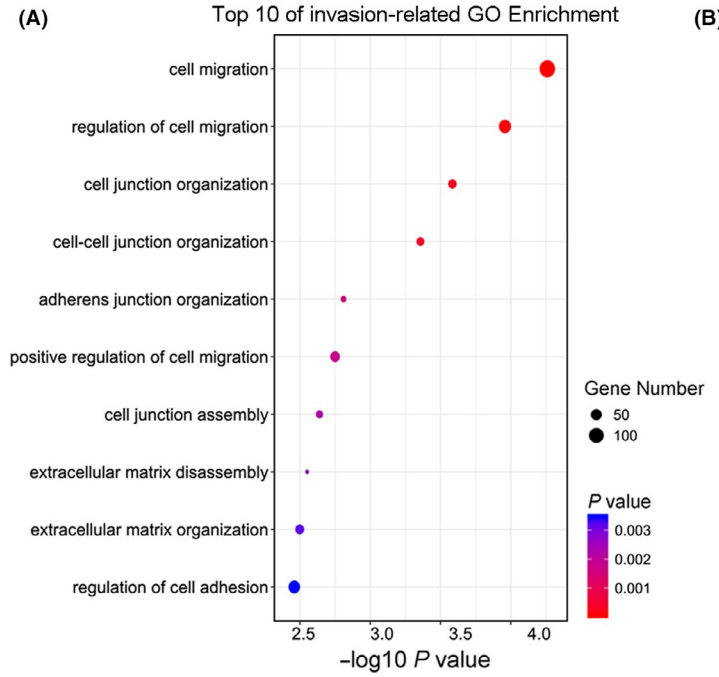

(B)

GO enrichment pathway	Related genes
cell migration	*PODXL2, NTN1, GNA12, MCAM, EPHB3, RAB11A, S100A7, LCP1, IL1A, ADAM8*
regulation of cell migration	*NTN1, GNA12, MCAM, RAB11A, S100A7, IL1A, ADAM8, SNAI1, PADI2, VEGFA*
cell junction organization	*FLNC, KRT14, SNAI1, VEGFA, CLDN3, PLEKHA7, FBF1, WNT4, GJD3, CDH1*
cell-cell junction organization	*SNAI1, VEGFA, PLEKHA7, CLDN3, GJD3, FBF1, WNT4, LAMA5, NECTIN1, CDH1*
adherens junction organization	*WNT4, VEGFA, PLEKHA7, LAMA5, NECTIN1, CAMSAP3, BCAS3, MMP14, CDH1, PPM1F*
positive regulation of cell migration	*MCAM, RAB11A, S100A7, IL1A, ADAM8, SNAI1, VEGFA, HBEGF, F3, CYR61*
cell junction assembly	*FLNC, KRT14, SNAI1, VEGFA, CLDN3, FBF1, WNT4, GJD3, LAMA5, BCAS3*
extracellular matrix disassembly	*LCP1, ADAM8, MMP1, MMP7, TIMP2, TGFB1, LAMC2, MMP14, CDH1, CD44*
extracellular matrix organization	*LCP1, ADAM8, CD47, CTGF, MMP7, CDH1, COL9A2, SERPINF2, CYR61,*
regulation of cell adhesion	*TGM2, EPHB3, IL20RB, IL4R, ADAM8, CD276, CD47, IL1B, VEGFA, CDH1*

FIGURE 4 Dysregulated signaling pathways in homeodomain-interacting protein kinase 2 (HIPK2)-attenuated cells. A, Gene Ontology (GO) analysis identified the top 10 enriched invasion-related pathways based on the dysregulated genes in Cal-27 cells with suppressed HIPK2. The size of the circle indicates the corresponding involved gene numbers; the color of the corrected*P*value indicates the significance of the enriched factors. B, Top 10 specific related genes in the top 10 GO enriched invasion-related signaling pathways.*CDH1*,*WNT4*, and*SNAI1*, the three genes of interest and most relevant to epithelial-mesenchymal transition, were chosen for further research (shown in red)

3.7 | Nuclear delocalization of HIPK2 associated with deficient P53 and E-Cad expression

To identify whether nuclear delocalization of HIPK2 was closely related to the changes in P53 and E-Cad expression, immunofluorescence analysis was used to investigate the cellular localization and expression of HIPK2, P53, and E-Cad in five OSCC cell lines and a normal epithelial cell line (HIOEC). The nuclear delocalization of HIPK2 was observed in four OSCC cell lines (SCC-9, UM-SCC-23, SCC-25, and HSC3), with remarkable cytoplasmic relocalization (Figure 6A). Consistently, the fluorescence of P53 and E-Cad was barely discernible in these cell lines (Figure 6B,C). A strong nuclear localization was observed only in the Cal-27 cell line (Figure 6A), which showed extensive nuclear positivity for P53 and continuous membrane staining of E-Cad (Figure 6B,C). Correlation analysis showed that HIPK2 expression ratio of nucleus to cytoplasm was positively correlated with E-Cad expression (Figure 6B) and P53 expression (Figure 6C) in OSCC cell lines. Additionally, Cal-27 cells with depletion of HIPK2 showed decreased HIPK2 nuclear localization staining and diminished fluorescence of P53 and E-Cad (Figure 7).

3.8 | Homeodomain-interacting protein kinase 2-mediated P53 targeting to CDH1 promoter

P53 acts as a guardian of epithelial integrity,[38,39] but its biological significance in *CDH1* transcription remains unclear. According to the PROMO and JASPAR databases, the promoter sequence of *CDH1* was predicted to contain several P53 binding sites. Thus, to identify whether P53 could directly target the *CDH1* promoter and activate its transcription, as triggered by HIPK2, four *CDH1* promoter sequences, each containing highly matched P53 binding sites, were each amplified and inserted into pSiCheck-2 for a dual-luciferase reporter assay (Figure 8A). In the pSiCheck-2-*CDH1* promoter-3/-4 group, increased or suppressed HIPK2 expression significantly activated or inhibited the luciferase reporter activity in a dose-dependent manner. When the P53-specific target seeds in the *CDH1* promoter-3/-4 were mutated, promoter activation or inhibition was restored (Figure 8B,C).

3.9 | Restoring P53 expression rescued E-Cad suppression induced by HIPK2 deficiency

To further verify whether attenuated HIPK2 suppressed *CDH1* transcription through P53 inhibition, we forced P53 expression in HIPK2-deficient cells to restore luciferase activity of the *CDH1* promoter. The results showed that increased P53 expression rescued the decreased luciferase activity of the *CDH1* promoter-3/-4 induced by HIPK2-sh in a dose-dependent manner (Figure 9A). Consistently, the restoration of P53 expression reversed the expression of E-Cad protein in Cal-27-HIPK2-sh cells (Figure 9B). Consequently, the enhanced tumor cell invasion ability triggered by attenuated HIPK2 was reduced (Figure 9C).

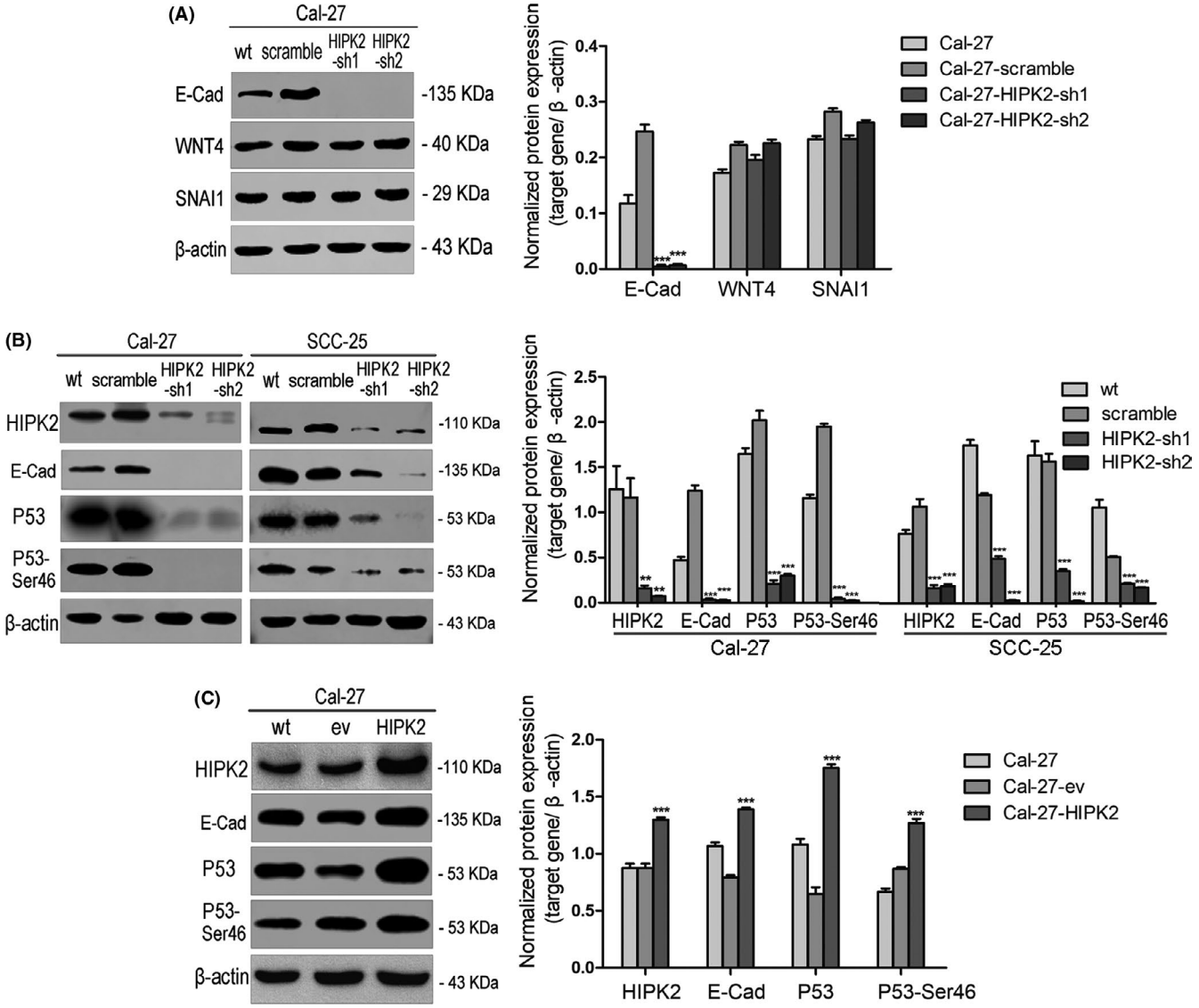

FIGURE 5 Homeodomain-interacting protein kinase 2 (HIPK2) regulated the expression of epithelial-mesenchymal transition (EMT) signaling genes. A, Protein levels of EMT-related genes (E-cadherin [E-Cad], WNT4, and SNAI1) in Cal-27-HIPK2-sh cells. B, C, Protein levels of HIPK2, E-Cad, P53, and P53-Ser46 in (B) Cal-27-/SCC-25-HIPK2-sh cells and (C) Cal-27-HIPK2 cells. $^{**}P < .01$; $^{***}P < .001$

3.10 | Restoring cytoplasmic HIPK2 expression in Cal-27 cells had no influence on the E-Cad expression or tumor cell invasion

According to a previous report, mutations of KK796/798AA, R826A, and K828E in HIPK2 nuclear localization sequences forced cytoplasmic localization of HIPK2.[40] Therefore, to elucidate the function of HIPK2 in cytoplasm, the cytoplasmic HIPK2 expression was rescued by transduction of flag-HIPK2 KK776/778AA, flag-HIPK2 R806A, or flag-HIPK2 K808E sequences into Cal-27 cells (Figure 10A). The immunofluorescence assay showed that Cal-27-flag-HIPK2 K808E cells exhibited exclusively cytoplasmic flag-HIPK2 expression (Figure 10B), whereas Cal-27-flag-HIPK2 KK776/778AA cells and Cal-27-flag-HIPK2 R806A cells presented universal nuclear and cytoplasmic localization (Figure S2). Thus, PCDH-flag-HIPK2 K808E vectors were used for further rescue experiments. The restoration of cytoplasmic HIPK2 expression in Cal-27 cells had no influence on the protein expression levels of E-Cad, P53, or P53-Ser46 (Figure 10C), nor on the tumor cell invasion ability (Figure 10D).

4 | DISCUSSION

In this study, we undertook a comprehensive investigation of HIPK2 expression modes in paired adjacent normal epithelia, dysplastic epithelia, OSCC tissue, and LM samples. It was found that HIPK2 was mainly localized in the nuclei of normal epithelia. During the process of carcinogenesis, two novel characteristics of HIPK2 expression were observed. One was that HIPK2 partially

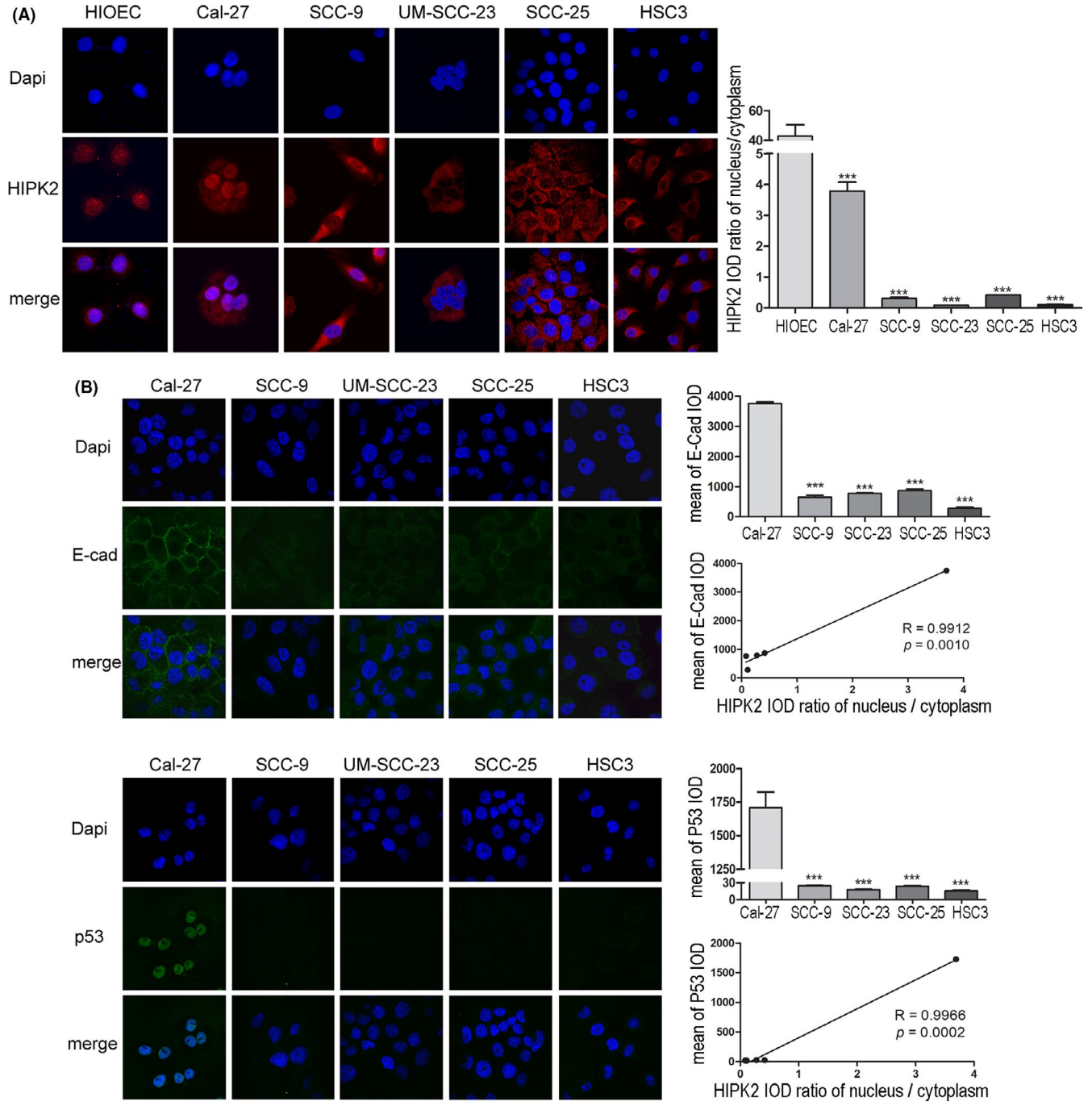

FIGURE 6 Nuclear delocalization of homeodomain-interacting protein kinase 2 (HIPK2) was associated with deficient P53 and E-cadherin (E-Cad) expression in oral squamous cell carcinoma cell lines. A, Representative immunofluorescence images show the nuclear localization of HIPK2 in HIOEC and Cal-27 cells, and the nuclear delocalization of HIPK2 in SCC-9, UM-SCC-23, SCC-25, and HSC3 cells. Cell nuclei were counterstained with DAPI (blue); HIPK2 protein is indicated by red staining. Original magnification, ×100. B, C, Immunofluorescence images of (B) P53 and (C) E-Cad in Cal-27, SCC-9, UM-SCC-23, SCC-25, and HSC3 cells. P53 and E-Cad proteins are indicated by green staining. Original magnification, ×100. HIPK2 fluorescence ratio of nucleus to cytoplasm / E-Cad correlation (B) and HIPK2 fluorescence ratio of nucleus to cytoplasm / P53 correlation (C) were determined by Pearson correlation. ***$P < .001$

or totally translocated from the cell nucleus to the cytoplasm. Further analysis revealed that the diminished nuclear localization of HIPK2 was related to poor clinicopathological factors and an unfavorable 5-year survival. These findings were in accordance with previous studies, which showed that the inactivation of nuclear HIPK2 in breast cancer[34,41] and leukemia[42] caused impairment in antitumor function. Therefore, diminished nuclear localization might be the key to inactivate HIPK2 in the nucleus and might serve as a valuable negative biomarker for poor prognosis in OSCC.

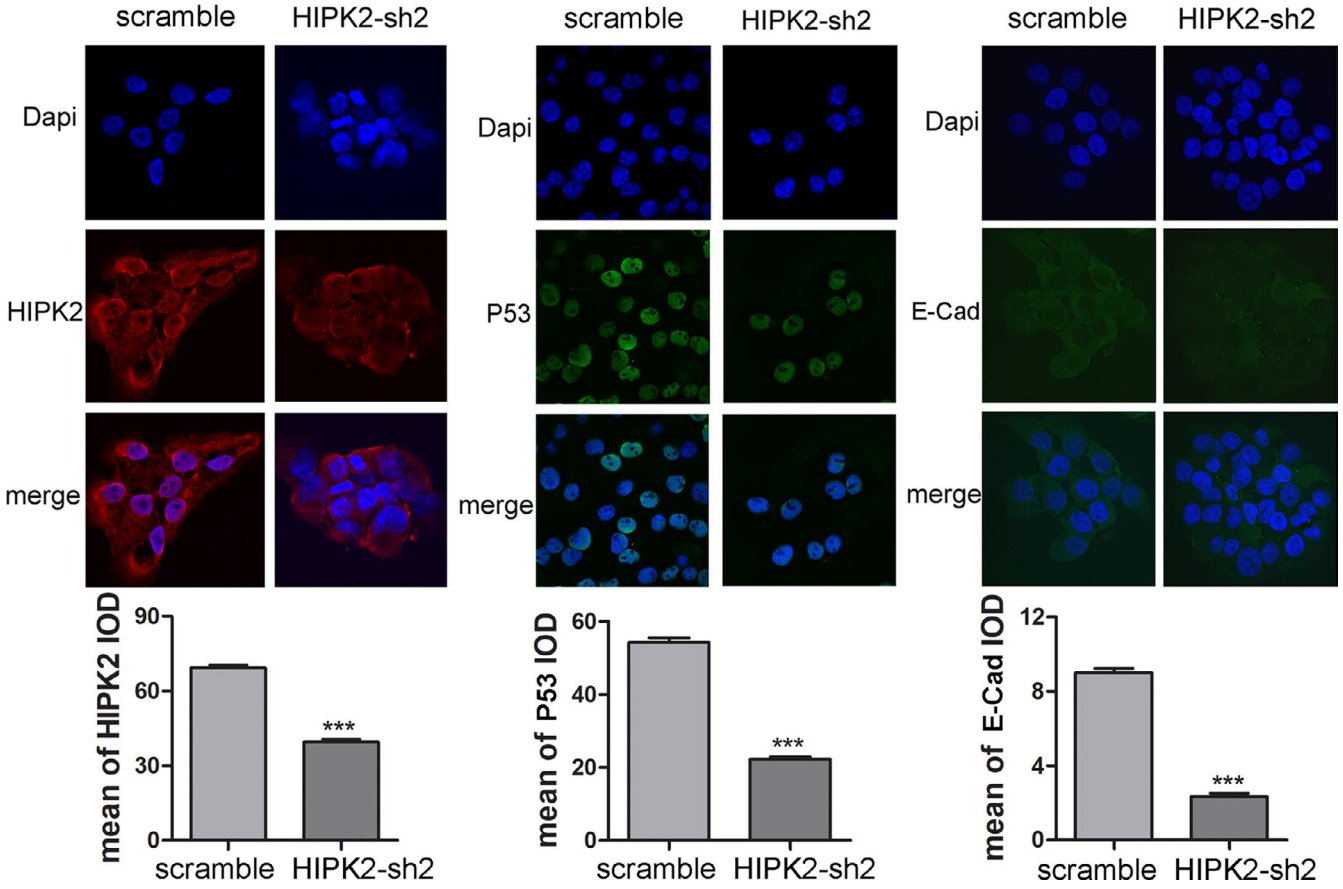

FIGURE 7 Attenuated homeodomain-interacting protein kinase 2 (HIPK2) decreased HIPK2 nuclear localization and the expression of P53 and E-cadherin (E-Cad). Immunofluorescence assays showed that Cal-27 cells with HIPK2 depletion exhibited decreased HIPK2 nuclear localization staining (left) and diminished fluorescence of P53 (middle) and E-Cad (right). Original magnification, ×100. Integrated optical density (IOD) mean values of HIPK2, P53, and E-Cad in Cal-27-HIPK2-sh2 cells were significantly lower than those in sh-scramble cells. ***$P < .001$

According to our results, the other feature of HIPK2 was its aberrant expression, which was elevated in tumor cells compared with normal epithelia, but decreased in most cases of metastasis compared with nonmetastasis. The HIPK2 dysregulation (both over- and underexpression) observed in this study was compatible with the findings presented by Saul and Schmitz,[11] in that only optimal amounts of HIPK2 were functional. This implies that higher concentrations of HIPK2 are less active, possibly due to the formation of inactive protein aggregates or misfolded HIPK2. Thus, overexpression of HIPK2 in OSCC might override protective mechanisms and induce malignant changes in cells. To further identify this "optimum model," more experimental evidence should be provided in the future.

On the contrary, our results showed a close correlation between decreased HIPK2 expression and OSCC LM. Further studies have reported that HIPK2 inhibited OSCC cell invasion ability in vitro and significantly impaired the capacity of these cells to generate LM in vivo. These results suggested an effective function of HIPK2 deficiency in promoting tumor metastasis. Although previous studies have confirmed that suppressing HIPK2 mediates tumor invasion and metastasis in several malignancies,[15,31-33] the mechanisms are not well defined. To our knowledge, only two signaling pathways involved in HIPK2 that oppose tumor invasion have been reported, including suppressing β4 integrin transcription[43] and promoting β-catenin nuclear localization.[15] Here, several signaling pathways and markers associated with tumor invasion and EMT were revealed in HIPK2-deficient cells. Notably, E-Cad expression was conspicuously inhibited by depletion of HIPK2. In accordance with our results, the decreased E-Cad in HIPK2-suppressed cells has also been found in esophageal SCC,[32] breast cancer,[33] and bladder cancer.[15] Therefore, all these findings strongly suggested the essential suppressor role of HIPK2 in inhibiting EMT by triggering E-Cad expression.

E-Cadherin, which is one of the most important adhesion molecules, plays a vital role in the maintenance of epithelial integrity,[44] and its repression increases EMT and tumor invasion.[45,46] In this study, we revealed a novel mechanism in which HIPK2 promoted P53-dependent E-Cad expression in OSCC. Homeodomain-interacting protein kinase 2 is widely known as a P53 activator and could maintain P53 native conformation.[47] It colocalizes and interacts with P53 and CREB-binding protein

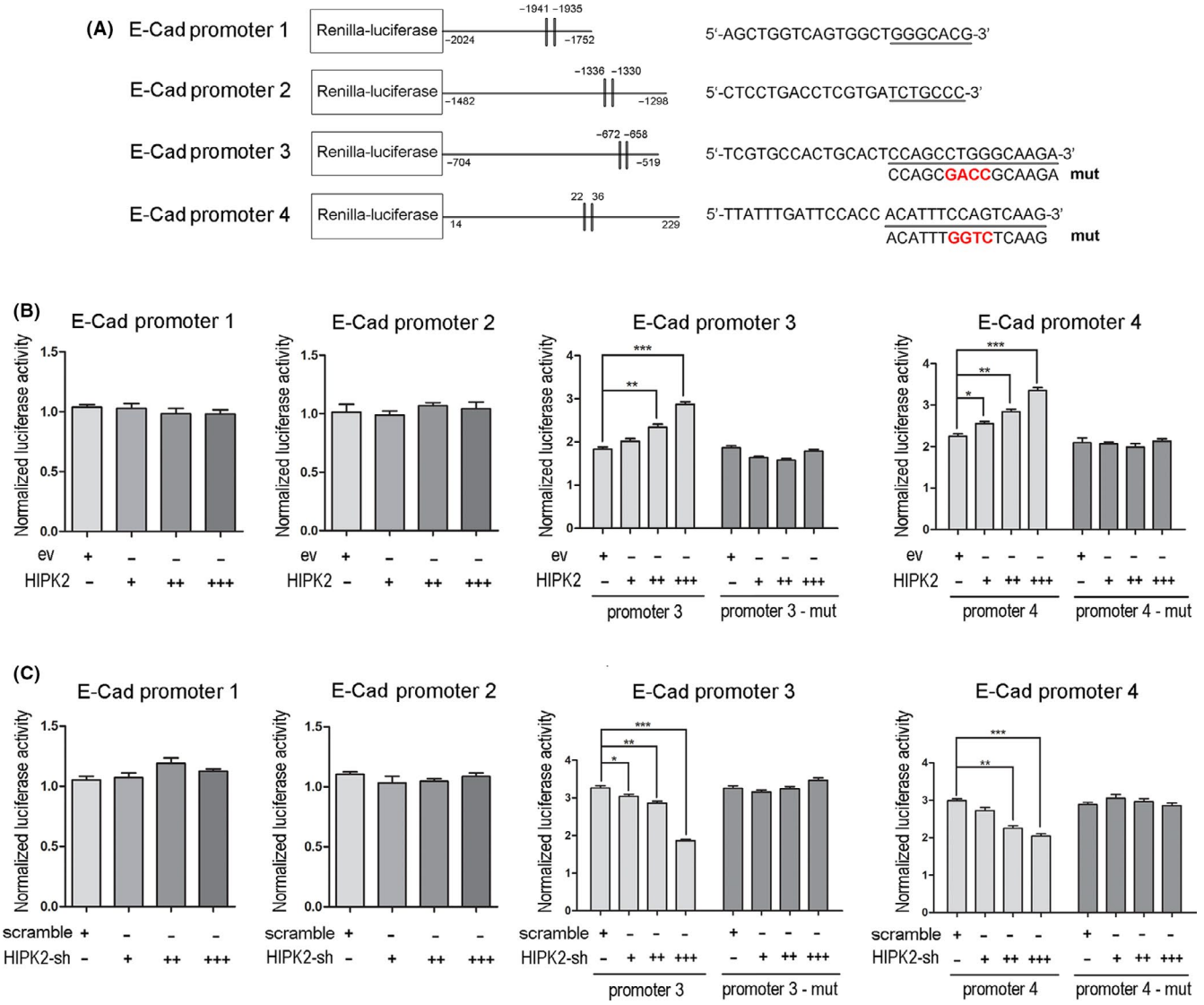

FIGURE 8 Homeodomain-interacting protein kinase 2 (HIPK2) mediated P53 targeting to the*CDH1* promoter. A, Diagram of four *CDH1* promoter fragments containing P53 binding sites (vertical lines). Underline indicates specific binding sequences; red sequences represent mutant bases. B, For the HIPK2-overexpressing luciferase reporter assays, 50 ng pSiCheck-2 vectors, pSiCheck-2-*CDH1* promoter-1/-2/-3/-4 vectors, or corresponding mutant vectors were transiently cotransfected with empty vector PCDH-EF1-puro plasmid or PCDH-EF1-HIPK2 plasmid into HSC3 cells (+, 50 ng; ++, 150 ng; +++, 300 ng; 96-well plate; 48 h transfection). In each ev group or HIPK2-ov group,*Renilla*luciferase activity was normalized to firefly luciferase activity, and then the final luciferase activity was normalized by pSiCheck-2-*CDH1* promoter/pSiCheck-2 or pSiCheck-2-*CDH1* mut promoter/pSiCheck-2. C, For the HIPK2-knockdown luciferase reporter assays, 50 ng pSiCheck-2 vectors, pSiCheck-2-*CDH1* promoter-1/-2/-3/-4 vectors, or corresponding mutant vectors were transiently cotransfected with sh-scramble plasmid or GV-248-HIPK2-sh2 plasmid into Cal-27 cells (+, 50 ng; ++, 150 ng; +++, 300 ng; 96-well plate; 48 h transfection). In each scramble group or HIPK2-sh group,*Renilla*luciferase activity was normalized to firefly luciferase activity, and then the final luciferase activity was normalized by pSiCheck-2-*CDH1* promoter/pSiCheck-2 or pSiCheck-2-*CDH1* mut promoter/pSiCheck-2. $^{*}P < .05$; $^{**}P < .01$; $^{***}P < .001$. E-Cad, E-cadherin

(CBP) within promyelocytic leukemia (PML) nuclear bodies.[48,49] Homeodomain-interacting protein kinase 2 can phosphorylate P53 at serine 46, thus facilitating the CBP-mediated acetylation of P53 at lysine 382, disrupting binding of MDM2, and mediating the expression of P53 target genes.[29,30,50] Activated P53 can act as a guardian of epithelial integrity and a restrictor of epithelial cell plasticity.[39] For example, the prevailing mechanism by which P53 blocks EMT is the activation of the P53-miRNAs-EMT-transcription factor (TF) axis, such as when P53 inhibits SNAI1 by promoting microRNA-34a expression.[51] In contrast, P53 can bind to enhancer regions of the *CDH1* locus and oppose trimethylation of H3K27 to maintain its acetylation, thereby maintaining E-Cad expression in EMT-prone cells.[38] According to the PROMO and JASPAR databases, we found significant enrichment of the motifs for the binding of P53 in the promoter regions of *CDH1*. A series of luciferase assays found that HIPK2 could induce direct binding of P53 to the

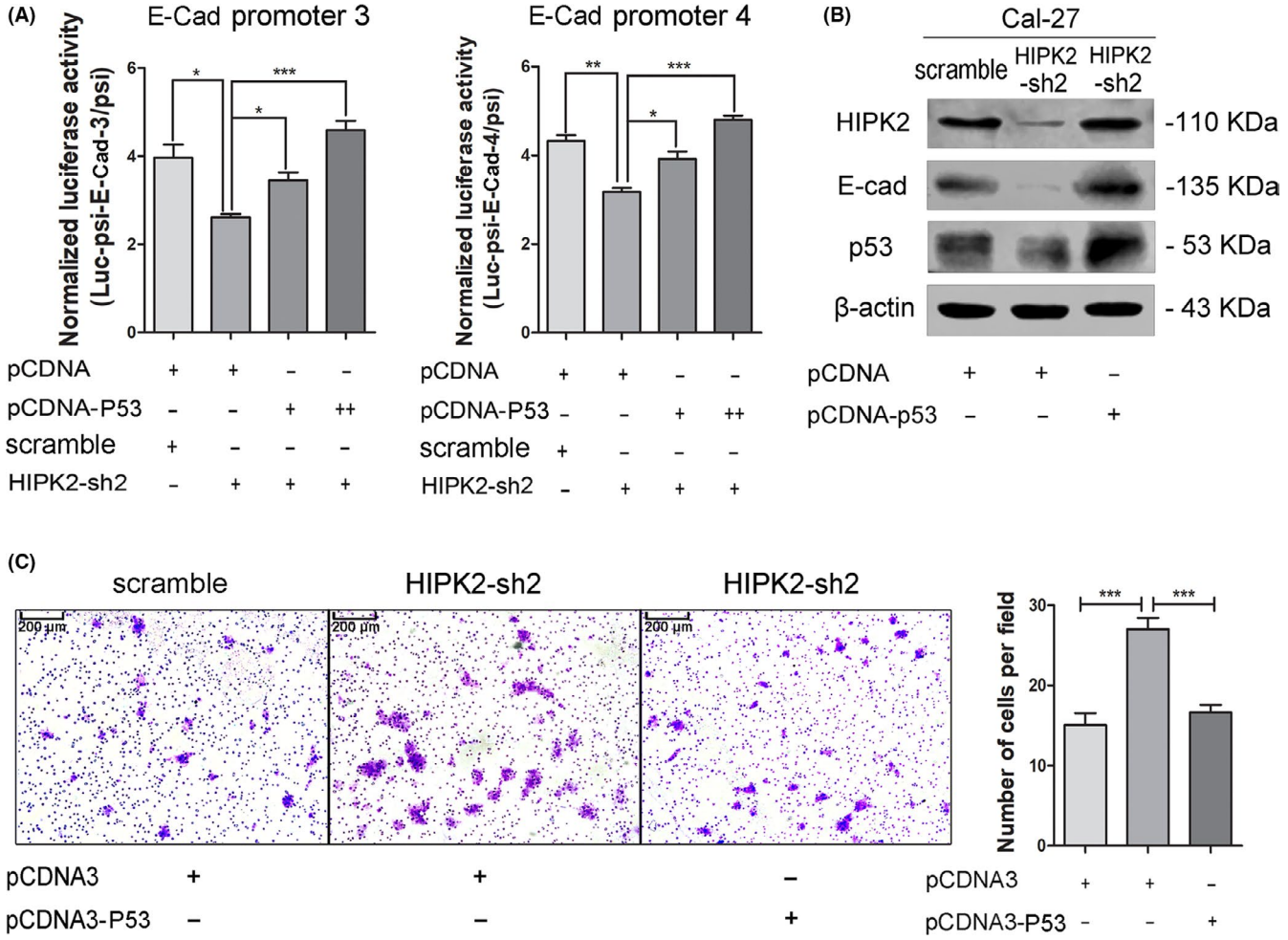

FIGURE 9 Restoring P53 expression rescued decreased E-cadherin (E-Cad) expression in the case of homeodomain-interacting protein kinase 2 (HIPK2) deficiency. A, For the P53-rescue in HIPK2-knockdown luciferase reporter assays, pCDNA3 plasmid, pCDNA3-P53 plasmid, sh-scramble plasmid, or GV-248-HIPK2-sh2 plasmid (+, 200 ng; ++, 300 ng, 96-well plate, 48 h transfection) were transiently cotransfected with pSiCheck-2 vectors or pSiCheck-2-*CDH1* promoter-1/-2/-3/-4 vectors (50 ng) into Cal-27 cells.*Renilla*luciferase activity was normalized to firefly luciferase activity. The final normalized luciferase activity was normalized by pSiCheck-2-*CDH1* promoter/pSiCheck-2. B, pCDNA3-P53 plasmid or pCDNA3 control plasmid was transfected into Cal-27-HIPK2-sh2 cells or sh-scramble cells, as indicated on thex-axis (2500 ng, 6-well plate). Then, 48 h after transfection, the protein levels of E-Cad and P53 were detected by western blotting. C, Transwell analysis of Cal-27-HIPK2-sh2 cells and sh-scramble cells that were transiently transfected with pCDNA3-P53 plasmid or pCDNA3 control plasmid (2500 ng, 6-well plate, 48 h transfection). The enhanced tumor cell invasion ability triggered by attenuated HIPK2 was significantly reduced by forced P53 expression. Original magnification, ×100. $^{*}P < .05$; $^{**}P < .01$; $^{***}P < .001$

promoter regions of the *CDH1* locus and then accelerate E-Cad transcription and expression. It was noted that the fold change of luciferase activity difference between control groups and experimental groups was not that remarkable, which might be attributed to the coordinated action of multiple TFs during the transcription regulation in eukaryotes. The transcriptional effect of factors binding to a single promoter site might be not particularly evident, whereas functional interactions between factors bound at multiple promoter sites on DNA often lead to a synergistic or more-than-additive transcriptional response. Here, we showed that the binding of P53 to the *CDH1* promoter region might be a novel underlying mechanism of HIPK2-mediated epithelial integrity in OSCC. However, the cooperative transcription factors and other synergistic binding promoter sites remain to be revealed by further research.

It is reported that HIPK2 disappearance from the nucleus may affect the multiprotein complex formation and inhibit P53 phosphorylation and transcriptional activity.[30] Our results further verified that the rescue of cytoplasmic HIPK2 expression had no influence on the P53/E-Cad axis or the tumor cell invasion ability. It suggests that HIPK2 might be activated in cell nucleus while inactivated in cytoplasm. Relocalization of HIPK2 from the nucleus to the cytoplasm resulted in the deprivation of HIPK2 antitumor function, thereby promoting OSSC progression.

Overall, the above results indicated that the nucleus delocalization of HIPK2 might serve as a valuable negative biomarker for OSCC poor prognosis and LM. The depletion of HIPK2 expression

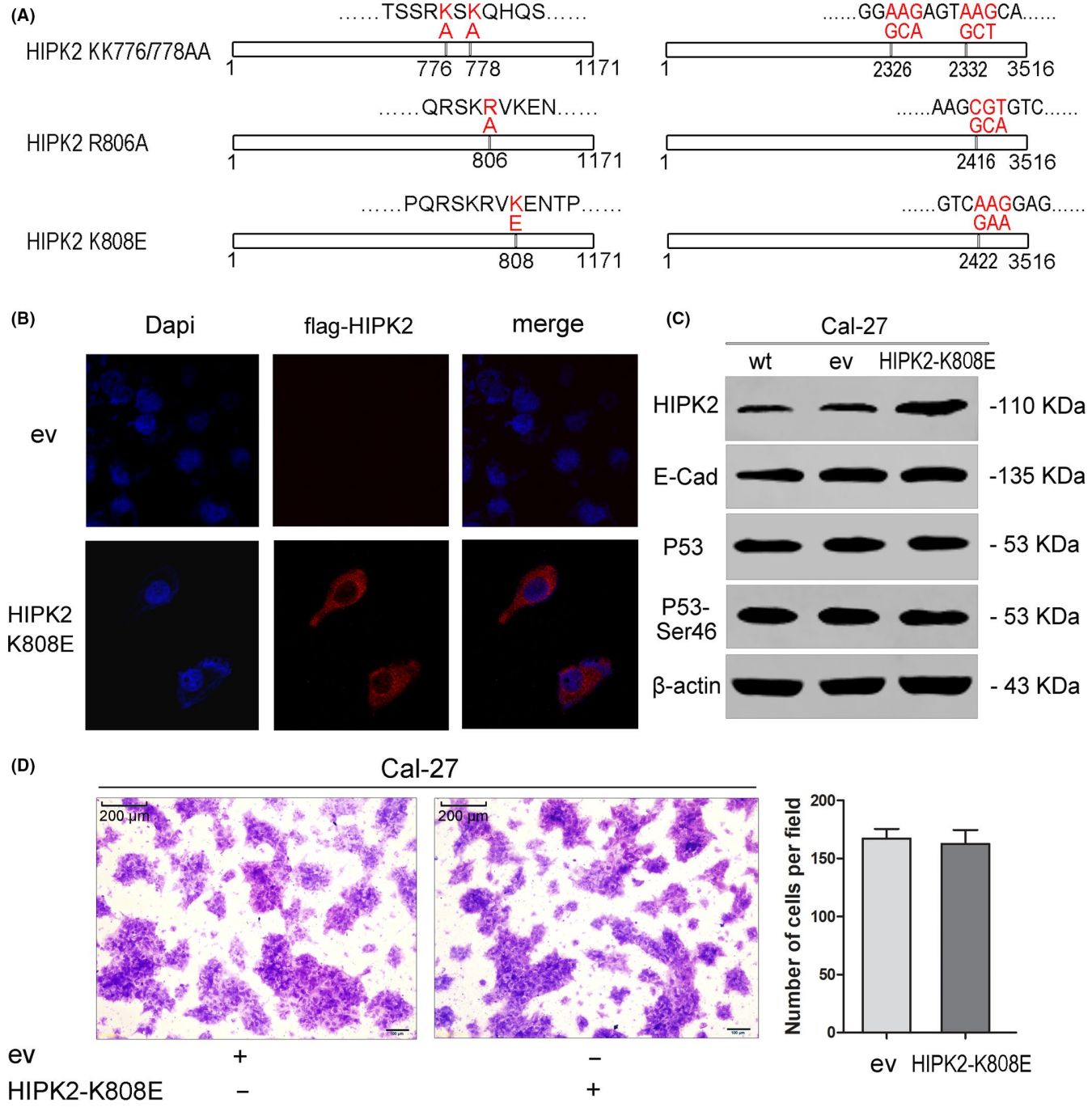

FIGURE 10 Restoring cytoplasmic homeodomain-interacting protein kinase 2 (HIPK2) expression in Cal-27 cells had no influence on the expression of E-cadherin (E-Cad) and tumor cell invasion. A, Schematic diagram of three HIPK2 nuclear localization sequence mutations of HIPK2 KK776/778AA, HIPK2 R806A, and HIPK2 K808E. The vertical line indicates the mutant position in the protein sequences (left) and bases sequences (right). Mutated amino acids and bases are shown in red. B, Representative immunofluorescence images of Cal-27 cells transiently transfected with 1000 ng PCDH-EF1-puro-flag empty vectors or PCDH-EF1-puro-flag-HIPK2 K808E vectors (12-well plate, 48 h transfection). Cell nuclei were counterstained with DAPI (blue); flag-HIPK2 protein is indicated by red staining. Original magnification, ×100. C, PCDH-EF1-puro-flag empty vectors or PCDH-EF1-puro-flag-HIPK2 K808E vectors were transiently transfected into Cal-27 cells (2500 ng, 6-well plate). Then, 48 h after transfection, protein expression levels of HIPK2, E-Cad, P53, and P53-Ser46 were detected by western blotting. D, Transwell analysis of Cal-27 cells transiently transfected with PCDH-EF1-puro-flag empty vectors or PCDH-EF1-puro-flag-HIPK2 K808E vectors (2500 ng, 6-well plate, 48 h transfection). Original magnification, ×100

would promote OSCC metastasis through suppressing the P53/E-Cad axis, which might be a promising target for anticancer therapies.

ACKNOWLEDGMENTS

We thank Mr Shichun Xiong and Ms Yuan Li of Wuhan University for their technical assistance. This work was supported by the

National Natural Science Foundation of China under Grant No. 81572664.

CONFLICT OF INTEREST

The authors have no conflict of interest.

DATA AVAILABILITY STATEMENT

All RNA-sequencing data supporting this article are accessible through NCBI's Gene Expression Omnibus accession number GSE158262.

ORCID

Jiali Zhang https://orcid.org/0000-0003-0965-3027

REFERENCES

1. Fan S, Tang QL, Lin YJ, et al. A review of clinical and histological parameters associated with contralateral neck metastases in oral squamous cell carcinoma. *Int J Oral Sci*. 2011;3:180-191.
2. Kim SY, Nam SY, Choi SH, Cho KJ, Roh JL. Prognostic value of lymph node density in node-positive patients with oral squamous cell carcinoma. *Ann Surg Oncol*. 2011;18:2310-2317.
3. Tankere F, Camproux A, Barry B, Guedon C, Depondt J, Gehanno P. Prognostic value of lymph node involvement in oral cancers: a study of 137 cases. *Laryngoscope*. 2000;110:2061-2065.
4. Sano D, Myers JN. Metastasis of squamous cell carcinoma of the oral tongue. *Cancer Metastasis Rev*. 2007;26:645-662.
5. Patel SG, Amit M, Yen TC, et al. Lymph node density in oral cavity cancer: results of the International Consortium for Outcomes Research. *Br J Cancer*. 2013;109:2087-2095.
6. Dumache R. Early diagnosis of oral squamous cell carcinoma by salivary microRNAs. *Clin Lab*. 2017;63:1771-1776.
7. Arellano-Garcia ME, Hu S, Wang J, et al. Multiplexed immunobead-based assay for detection of oral cancer protein biomarkers in saliva. *Oral Dis*. 2008;14:705-712.
8. Kim YH, Choi CY, Lee SJ, Conti MA, Kim Y. Homeodomain-interacting protein kinases, a novel family of co-repressors for homeodomain transcription factors. *J Biol Chem*. 1998;273:25875-25879.
9. Calzado MA, Renner F, Roscic A, Schmitz ML. HIPK2: a versatile switchboard regulating the transcription machinery and cell death. *Cell Cycle*. 2007;6:139-143.
10. Roscic A, Moller A, Calzado MA, et al. Phosphorylation-dependent control of Pc2 SUMO E3 ligase activity by its substrate protein HIPK2. *Mol Cell*. 2006;24:77-89.
11. Saul VV, Schmitz ML. Posttranslational modifications regulate HIPK2, a driver of proliferative diseases. *J Mol Med (Berl)*. 2013;91:1051-1058.
12. Calzado MA, de la Vega L, Moller A, Bowtell DD, Schmitz ML. An inducible autoregulatory loop between HIPK2 and Siah2 at the apex of the hypoxic response. *Nat Cell Biol*. 2009;11:85-91.
13. Hofmann TG, Glas C, Bitomsky N. HIPK2: a tumour suppressor that controls DNA damage-induced cell fate and cytokinesis. *BioEssays*. 2013;35:55-64.
14. Link N, Chen P, Lu WJ, et al. A collective form of cell death requires homeodomain interacting protein kinase. *J Cell Biol*. 2007;178:567-574.
15. Tan M, Gong H, Zeng Y, et al. Downregulation of homeodomain-interacting protein kinase-2 contributes to bladder cancer metastasis by regulating Wnt signaling. *J Cell Biochem*. 2014;115:1762-1767.
16. Lavra L, Rinaldo C, Ulivieri A, et al. The loss of the p53 activator HIPK2 is responsible for galectin-3 overexpression in well differentiated thyroid carcinomas. *PLoS One*. 2011;6:e20665.
17. Zhou L, Feng Y, Jin Y, et al. Verbascoside promotes apoptosis by regulating HIPK2-p53 signaling in human colorectal cancer. *BMC Cancer*. 2014;14:747.
18. D'Orazi G, Sciulli MG, Di Stefano V, et al. Homeodomain-interacting protein kinase-2 restrains cytosolic phospholipase A2-dependent prostaglandin E2 generation in human colorectal cancer cells. *Clin Cancer Res*. 2006;12:735-741.
19. Nardinocchi L, Puca R, Guidolin D, et al. Transcriptional regulation of hypoxia-inducible factor 1alpha by HIPK2 suggests a novel mechanism to restrain tumor growth. *Biochim Biophys Acta*. 2009;1793:368-377.
20. Yu J, Deshmukh H, Gutmann RJ, et al. Alterations of BRAF and HIPK2 loci predominate in sporadic pilocytic astrocytoma. *Neurology*. 2009;73:1526-1531.
21. Kwon MJ, Min SK, Seo J, et al. HIPK2 expression in progression of cutaneous epithelial neoplasm. *Int J Dermatol*. 2015;54:347-354.
22. Cheng Y, Al-Beiti MA, Wang J, et al. Correlation between homeodomain-interacting protein kinase 2 and apoptosis in cervical cancer. *Mol Med Rep*. 2012;5:1251-1255.
23. Wook Choi D, Yong CC. HIPK2 modification code for cell death and survival. *Mol Cell Oncol*. 2014;1:e955999.
24. de la Vega L, Grishina I, Moreno R, Kruger M, Braun T, Schmitz ML. A redox-regulated SUMO/acetylation switch of HIPK2 controls the survival threshold to oxidative stress. *Mol Cell*. 2012;46:472-483.
25. Feng Y, Zhou L, Sun X, Li Q. Homeodomain-interacting protein kinase 2 (HIPK2): a promising target for anti-cancer therapies. *Oncotarget*. 2017;8:20452-20461.
26. Polonio-Vallon T, Kirkpatrick J, Krijgsveld J, Hofmann TG. Src kinase modulates the apoptotic p53 pathway by altering HIPK2 localization. *Cell Cycle*. 2014;13:115-125.
27. Chiocca S, Seiser C. Lifting the threshold between life and death: SUMO and HDAC fine-tune HIPK2 to sense redox status. *Mol Cell*. 2012;46:382-383.
28. Sung KS, Lee YA, Kim ET, Lee SR, Ahn JH, Choi CY. Role of the SUMO-interacting motif in HIPK2 targeting to the PML nuclear bodies and regulation of p53. *Exp Cell Res*. 2011;317:1060-1070.
29. D'Orazi G, Cecchinelli B, Bruno T, et al. Homeodomain-interacting protein kinase-2 phosphorylates p53 at Ser 46 and mediates apoptosis. *Nat Cell Biol*. 2002;4:11-19.
30. Nardinocchi L, Puca R, Givol D, D'Orazi G. HIPK2-a therapeutical target to be (re)activated for tumor suppression: role in p53 activation and HIF-1alpha inhibition. *Cell Cycle*. 2010;9:1270-1275.
31. Tan X, Tang H, Bi J, Li N, Jia Y. MicroRNA-222-3p associated with Helicobacter pylori targets HIPK2 to promote cell proliferation, invasion, and inhibits apoptosis in gastric cancer. *J Cell Biochem*. 2018;119:5153-5162.
32. Zhang Z, Wen P, Li F, et al. HIPK2 inhibits cell metastasis and improves chemosensitivity in esophageal squamous cell carcinoma. *Exp Ther Med*. 2018;15:1113-1118.
33. Nodale C, Sheffer M, Jacob-Hirsch J, et al. HIPK2 downregulates vimentin and inhibits breast cancer cell invasion. *Cancer Biol Ther*. 2012;13:198-205.
34. Bon G, Di Carlo SE, Folgiero V, et al. Negative regulation of beta4 integrin transcription by homeodomain-interacting protein kinase 2 and p53 impairs tumor progression. *Cancer Res*. 2009;69:5978-5986.
35. Zheng X, Wu K, Liao S, et al. MicroRNA-transcription factor network analysis reveals miRNAs cooperatively suppress RORA in oral squamous cell carcinoma. *Oncogenesis*. 2018;7:79.
36. Bais MV, Kukuruzinska M, Trackman PC. Orthotopic non-metastatic and metastatic oral cancer mouse models. *Oral Oncol*. 2015;51:476-482.
37. Shirako Y, Taya Y, Sato K, et al. Heterogeneous tumor stromal microenvironments of oral squamous cell carcinoma cells in tongue and nodal metastatic lesions in a xenograft mouse model. *J Oral Pathol Med*. 2015;44:656-668.

38. Oikawa T, Otsuka Y, Onodera Y, et al. Necessity of p53-binding to the CDH1 locus for its expression defines two epithelial cell types differing in their integrity. *Sci Rep*. 2018;8:1595.
39. Oikawa T, Otsuka Y, Sabe H. p53-dependent and -independent epithelial integrity: beyond miRNAs and metabolic fluctuations. *Cancers (Basel)*. 2018;10(6):162.
40. de la Vega L, Frobius K, Moreno R, Calzado MA, Geng H, Schmitz ML. Control of nuclear HIPK2 localization and function by a SUMO interaction motif. *Biochim Biophys Acta*. 2011;1813:283-297.
41. D'Orazi G, Rinaldo C, Soddu S. Updates on HIPK2: a resourceful oncosuppressor for clearing cancer. *J Exp Clin Cancer Res*. 2012;31:63.
42. Wee HJ, Voon DC, Bae SC, Ito Y. PEBP2-beta/CBF-beta-dependent phosphorylation of RUNX1 and p300 by HIPK2: implications for leukemogenesis. *Blood*. 2008;112:3777-3787.
43. Munz M, Baeuerle PA, Gires O. The emerging role of EpCAM in cancer and stem cell signaling. *Cancer Res*. 2009;69:5627-5629.
44. Sakamoto K, Imanishi Y, Tomita T, et al. Overexpression of SIP1 and downregulation of E-cadherin predict delayed neck metastasis in stage I/II oral tongue squamous cell carcinoma after partial glossectomy. *Ann Surg Oncol*. 2012;19:612-619.
45. Yoshida R, Morita M, Shoji F, et al. Clinical significance of SIP1 and E-cadherin in patients with esophageal squamous cell carcinoma. *Ann Surg Oncol*. 2015;22:2608-2614.
46. Xie CG, Wei SM, Chen JM, et al. Down-regulation of GEP100 causes increase in E-cadherin levels and inhibits pancreatic cancer cell invasion. *PLoS One*. 2012;7:e37854.
47. Puca R, Nardinocchi L, Gal H, et al. Reversible dysfunction of wild-type p53 following homeodomain-interacting protein kinase-2 knockdown. *Cancer Res*. 2008;68:3707-3714.
48. Hofmann TG, Moller A, Sirma H, et al. Regulation of p53 activity by its interaction with homeodomain-interacting protein kinase-2. *Nat Cell Biol*. 2002;4:1-10.
49. Moller A, Sirma H, Hofmann TG, et al. PML is required for homeodomain-interacting protein kinase 2 (HIPK2)-mediated p53 phosphorylation and cell cycle arrest but is dispensable for the formation of HIPK domains. *Cancer Res*. 2003;63:4310-4314.
50. Rinaldo C, Prodosmo A, Mancini F, et al. MDM2-regulated degradation of HIPK2 prevents p53Ser46 phosphorylation and DNA damage-induced apoptosis. *Mol Cell*. 2007;25:739-750.
51. Kim NH, Kim HS, Li XY, et al. A p53/miRNA-34 axis regulates Snail1-dependent cancer cell epithelial-mesenchymal transition. *J Cell Biol*. 2011;195:417-433.

SUPPORTING INFORMATION

Additional supporting information may be found online in the Supporting Information section.

How to cite this article: Zheng X, Pan Y, Chen X, et al. Inactivation of homeodomain-interacting protein kinase 2 promotes oral squamous cell carcinoma metastasis through inhibition of P53-dependent E-cadherin expression. *Cancer Sci*. 2021;112:117–132. https://doi.org/10.1111/cas.14691